RSC Advances

ROYAL SOCIETY OF CHEMISTRY

www.rsc.org/advances

Comparative study on temperature/pH sensitive xylan-based hydrogels: Their properties and drug controlled release

Cundian Gao[a], Junli Ren *[a], Weiqing Kong[a], Runcang Sun[b], Qifeng Chen[a]

[a]*State Key Laboratory of Pulp and Paper Engineering, South China University of Technology, Guangzhou, 510640, Guangdong, China*

[b]*Beijing Key Laboratory of Lignocellulosic Chemistry, College of Materials Science and Technology, Beijing Forestry University, Beijing, 100083, China*

* Corresponding author. E-mail address: renjunli@scut.edu.cn

Current address: State Key Laboratory Pulp and Paper Engineering, South China University of Technology, Guangzhou, 510640, China.

Tel.: +86-20-87111861; Fax: +86-20-87111861.

Abstract

Temperature/pH dual-responsive hydrogels were prepared by the grafting copolymerization of xylan possessing different functional groups with *N*-isopropylacrylamide and acrylamide using *N,N′*-methylenebis-acrylamide as a cross-linker and 2,2-dimethoxy-2-phenylacetophenone as a photoinitiator via ultraviolet irradiation. The influence of xylan and glycidyl methacrylate-modified xylan (GMAX) as the raw materials on the mechanical properties of hydrogels was comparatively investigated. Hydrogels were characterized by SEM, FTIR, TGA and XRD. The prepared hydrogels demonstrated a rapid phase transition temperature around 35 ^{o}C. The cumulative release rate of acetylsalicylic acid for xylan-based hydrogels and GMAX-based hydrogels reached to 77.5% and 84.2% in the intestinal fluid, respectively. GMAX-based hydrogels had a drug encapsulation efficiency of 95.21% and low drug release rate in gastric fluid. NIH3T3 cells in GMAX-based hydrogels had the high cell viability by MTT essay. Therefore, GMAX-based hydrogels had the good biocompatibility which make them promising in biomedical applications, especially as intestinal-targeted drug carriers.

Keywords: Xylan; Glycidyl methacrylate modified xylan; Hydrogels; Temperature/pH sensitivity; Drug release; Biocompatibility

Introduction

Hydrogels are three-dimensional, cross-linked networks of hydrophilic polymers, which have variety of functional properties with both liquid-like and solid-like deformable features.[1-3] In recent years, stimuli-sensitive hydrogels as intelligent materials have attracted considerable attention in the biochemical and biomedical fields, such as tissue engineering,[4,5] cellular immobilization[6] and drug controlled delivery.[7,8] Among the multiple stimuli-sensitive hydrogels, temperature and pH sensitive hydrogels have received much attention in the biomedical field especially in the drug controlled release system because temperature and pH are essential and crucial environmental conditions for some diseases and are also controllable and applicable in vitro and in vivo.[9] Moreover, temperature and pH sensitive hydrogels for drug delivery could prolong the retaining time of drug and reduce side effects of drugs by the volume phase transition with the external stimuli.[7]

The poly(*N*-isopropylacrylamide) (PNIPAm) hydrogel is one of the most studied temperature sensitive hydrogels with a lower critical solution temperature (LCST) around 33 ^{o}C, which makes it suitable for drug controlled delivery because the phase transition temperature is close to human body temperature.[8,10,11] Many researchers have attempted to copolymerize PNIPAm with charged co-monomers, such as methacrylic acid and ethyl glycinate, which endowed the copolymer with the pH and temperature sensitivity.[12,13] Tanaka *et al.* firstly reported pH sensitive hydrogels and clarified the role of ionization in the phase transitions of gels.[14] From then on, many researchers had paid extensive focus on preparing pH sensitive hydrogels by introducing radicals or carboxylic acid groups which were easily ionized.[15-17] However, PNIPAm and polyacrylamide (PAM) hydrogels have a fatal defect of weak strength. Their degradation monomers are toxic and incompatible with human organs

and tissues, which limit their application in the biomedical fields. These obstacles could be overcome by interpenetrating them with natural polymers such as chitosan,[18,19] cellulose,[20] and pullulan[9] due to the good biocompability of biomass materials. Introducing natural polymers into PNIPAm chains would facilitate the binding affinity and biocompatibility with human tissues. In addition, natural polymers-based PNIPAm hydrogels had the remarkable structural stability and there was not toxic monomers from hydrogels degradation in the most studies.[21,22] This could be explained by the fact that incorporating PNIPAm onto natural polymers with active hydroxyl groups could build the stable network structure resulting from due to the formation of strong hydrogen bonds. These natural polymers with a great amount of hydrophilic hydroxyl groups also have positive effects on the stimuli-responsive behavior of hydrogels. Moreover, hydrogels with the temperature response still have a relatively low LCST. The addition of hydrophilic biopolymers and monomers (such as AM) could increase the intermolecular forces of hydrogel networks because of the formation of hydrogen bonds and then further improved the phase transition temperature of PNIPAm hydrogels.[23] It is desirable for the application in human oral drug carriers.

Xylan is the major component of hemicelluloses which are the second abundant biopolymer next to cellulose in nature. It is also the major non-cellulosic cell wall polysaccharide of cereals, grasses, and angiosperms which are available from agricultural byproducts and plant resources. The function of xylan has been explored in various industrial and biomedical applications.[24] Recently, more attentions have been paid to the application of xylan for drug delivery and tissue engineering due to their innate immunity and antioxidant properties.[25] Xylan-based hydrogels or other functional biomaterials have aroused public concern not only because of the

properties of non-toxicity, abundance and biodegradability of xylan,[12,24,26,27] but also because of its particular physiological characteristics which show unique and competitive advantages, including biocompatibility, inhibiting cell mutation and anti-cancer effect, etc.[28,29] Hromadkova *et al.* investigated the property of xylan isolated from corn cobs and suggested that xylan was applicable as an additive in the pharmaceutical industry.[30] Furthermore, xylan based hydrogels have been proved to be suitable for sustained targeted release of encapsulated products in the human digestive system because xylan was chemo-stable and resistant to digestion in the human stomach and intestine.[31] Spruce xylan-based hydrogels which were prepared by enzymatic crosslinking had the promising application in the cell immobilization. Xylan could be as a promising precursor to prepare in situ forming hydrogels for tissue engineering.[32] Xylan-rich hemicelluloses-graft-acrylic acid ionic hydrogels showed rapid and multiple responses to pH, ions, and organic solvents, which may allow their use in medicine delivery systems.[33] The pH-sensitive hemicelluloses-graft-acrylic acid biodegradable hydrogels used for controlled drug delivery were investigated by Sun *et al.*[17] Acetylsalicylic acid and theophylline were comparatively studied as drug models. Results showed that acetylsalicylic acid had higher cumulative release amount, which indicated the drug release behavior was controlled both by hydrogels and drugs.

To increase the reactivity of xylan, alkenyl groups were introduced onto the backbone structure of xylan-type hemicelluloses in most studies which facilitated the crosslinking reaction and copolymerization with other monomers to prepare biocompatible macromolecular copolymers.[26,33-35] Glycidyl methacrylate (GMA) modified biopolymers (dextran, hyaluronic acid, alginate) which are highly compatible with vascular smooth muscle cells have been utilized as raw materials for

the preparation of hydrogels and showed promising applications in drug delivery and tissue engineering.[36,37] These results proved that GMA modified biopolymers had high compatibility and nontoxicity, and also had the great reactivity. Peng *et al.* introduced methacryloyl groups onto xylan-type hemicelluloses successfully by the transesterification reaction of xylan-type hemicelluloses with GMA in dimethyl sulfoxide (DMSO).[38] And then new photo-responsive hydrogels were prepared by the free radical copolymerization of GMA-modified xylan-type hemicelluloses with 4-[(4-acryloyloxyphenyl)azo]benzoic acid (AOPAB),[26] these hydrogels showed multi-responsive behaviors to pH, water/ethanol alternating solutions and light, which were indicative of an promising application in the light-controlled drug delivery system. Most pH sensitive hydrogels are attributed to grafting carboxylic acid groups. Nevertheless, the hydrophilic macromolecules themselves with a large amount of active hydroxyl groups in hydrogels also showed the pH sensitivity.[39] Different functional groups impart xylan with various properties which have important impacts on the network structure of hydrogels and consequently would affect their application.

Acetylsalicylic acid is an anti-inflammatory hydro-soluble pain killer and has been extensively used as anti-platelet drug for the prevention of cardiovascular events.[40,41] However, acetylsalicylic acid has common side-effects including gastric irritation, nausea and vomiting. It could even lead to gastric ulcer, gastrorrhagia and salicylism for patients with long-term drug use.[42,43] Therefore, intestinal-targeted drug carrier hydrogels were considered to carry acetylsalicylic acid and to reduce drug release in gastric fluid. This was beneficial to reduce side-effects of acetylsalicylic acid.

In view of these facts mentioned above, the properties and the acetylsalicylic acid release behavior of intestinal-targeted xylan-based temperature/pH dual-responsive Poly (AM-co-NIPAm) hydrogels by the grafting copolymerization under ultraviolet

(UV) irradiation were investigated in this study. Introduced methacryloyl groups could endow xylan with higher reactivity due to the presence of alkenyl groups, which facilitated the grafting copolymerization of xylan with AM and NIPAm. As a result, the influence of xylan and GMA modified xylan (GMAX) as the raw materials on the properties and applications of xylan based hydrogels (xylan-gels) and GMAX based hydrogels (GMAX-gels) was discussed by comparing the swelling ratio, the mechanical properties, drug loading, loading efficiency and drug release. Xylan-gels and GMAX-gels were prepared under the same conditions, and 2, 2-Dimethoxy-2-phenylacetophenone (DMPA) as an efficient and stable UV photosensitizer was employed. UV initiator was used because it had higher efficiency and lower toxicity than other redox chemicals. The phase transition temperature of these two types of hydrogels was determined by differential scanning calorimetry (DSC), which reflected the temperature sensitivity of hydrogels as well as the differences between Poly(AM-co-NIPAm) hydrogels and PNIPAm hydrogels (LCST, about 33 ^{o}C). A comparative study was conducted to investigate the characterizations of xylan and GMAX based multi-sensitive hydrogels by scanning electron microscopy (SEM), Fourier transform infrared spectroscopy (FTIR), thermogravimetric analysis (TGA) and X-ray diffraction (XRD). The biocompatibility of xylan-based hydrogels was evaluated using NIH3T3 cells by MTT assay.

Materials and methods

Materials

Beech wood xylan (M_w of 130, 000 g/mol) was purchased from Sigma Aldrich (Germany) and used without further purification. NIPAm (98%), *N,N′*-methylenebis-acrylamide (MBA, 98%), AM (98%), GMA (98%), NaCl,

dimethylaminopyridine (DMAP, 99%), DMSO (98%), acetylsalicylic acid (99%) were supplied by Aladdin Reagent Company Limited (Shanghai, China). Mouse embryonic fibroblasts (NIH3T3 cells) were achieved from School of Bioscience and Bioengineering, South China University of Technology (Guangzhou, China), 3-(4,5-dimethylthiazol-2-yl)-2,5-diphenyltetrazolium bromide (MTT) was obtained from Sigma-Aldrich (St. Louis, MO), Fetal bovine serum (FBS) was purchased from Si Jiqing Bio-engineering Material Company (Hangzhou, China), DMPA (99%) and *N*-methyl pyrrolidone (NMP, 99%) were obtained from Guangzhou Chemical Reagent Factory (Guangzhou, China). All chemical reagents used were analytical reagent grade. Deionized water was used in the preparation of hydrogels.

Preparation of glycidyl methacrylate modified xylan (GMAX)

The procedure of GMAX synthesis was carried out according to the literature under the optimal condition.[38] 0.66 g of xylan was dissolved in DMSO (30 ml) and the mixture was stirred for 1.5 h at 95 ^{o}C. After xylan was dissolved completely, the solution was cooled down to room temperature, and then 0.132 g of DMAP (20 wt%, base on the weight of xylan) as the catalyst was added to the solution, followed by stirring at 40 ^{o}C for 0.5 h. Subsequently, 1.32 g of GMA was added, and the mixture was stirred at 40 ^{o}C for 36 h. Eventually, the resulting solution was precipitated in 150 ml of ethanol (95%, w/w) and centrifuged to remove the unreacted reagents. The precipitates were dissolved in deionizead water after ethanol volatilization and then freeze-dried at -70 ^{o}C in the vacuum freeze dryer (FM25XL-70, USA). The resulting products were grinded into powder for the subsequent preparation of GMAX-gels. The degree of substitution (DS) of GMAX was achieved up to 0.94. The DS was determined by percentages of C, H, and O of the product detected by the elemental

analysis.[44] All samples were grinded into powder and dried at 60 °C for 24 h before determination. Carbon content in GMAX sample was measured to determine the DS.[45] The DS values were calculated as follow:

$$DS = \frac{C\% \times 132 - 60}{48 - 69 \times C\%} \quad (1)$$

where C% is the carbon content of product determined by the elemental analysis. 132 and 69 are the molecular weights ($g \cdot mol^{-1}$) of xylose unit in xylan and the methacryloyl group. 60 and 48 are the total molecular weights ($g \cdot mol^{-1}$) of carbon element in xylose unit and methacryloyl group respectively.

Preparation of xylan-gels and GMAX-gels

Table 1 Synthesis conditions, compressive modulus, drug loading and encapsulation efficiency of xylan-gels and GMAX-gels.

Xylan-gels		GMAX-gels	
NIPAm/xylan (g/g)	0.1	NIPAm/GMAX (g/g)	0.1
AM/xylan (g/g)	5	AM/GMAX (g/g)	5
MBA/xylan (g/g)	0.1	MBA/GMAX (g/g)	0.1
Initiator (%)	2.5	Initiator (%)	2.5
Compressive modulus (kPa)	105.17±5.65	Compressive modulus (kPa)	156.78±9.54
Drug loading (%)	28.65±1.25	Drug loading (%)	35.56±2.15
Encapsulation efficiency (%)	64.46±3.24	Encapsulation efficiency (%)	95.21±2.67

Xylan-based hydrogels were prepared by the grafting polymerization under UV irradiation. A predetermined amount of xylan (or GMAX) was dissolved in the distilled water at a concentration of 5% (w/w) and the solution was stirred and heated at 85 °C for 0.5 h, then the system temperature was dropped to 50 °C. NIPAm, AM, and MBA as a crosslinker were added. After bubbling N_2 for 15 min, DMPA (5% w/w, based on dried xylan or GMAX weight) which was firstly dissolved in the NMP solution to form the 2.5% w/w concentration, was added as a photosensitizer. The

detailed synthesis conditions are shown in Table 1. The solution was poured into a teflon mould and irradiated under the ultraviolet light (365 nm and 40 W) at room temperature for 6 h after the mixture was homogeneous. Subsequently, the samples were well-sealed at room temperature for 12 h to further keep polymerization and crosslinking of polymer networks completely. After then, the samples were removed and washed thoroughly in deionized water for 5 days. Meanwhile, the deionized water was refreshed 6 times daily to remove the impurities and unreacted chemicals. Finally, the obtained hydrogels were cut into slices (about 8 mm length, 8 mm width and 2 mm thickness) and dried at -70 ^{o}C in the vacuum freeze dryer. The samples were dried to constant weight in a vacuum oven and stored in a desiccator before testing. The preparation scheme of xylan-gels and GMAX-gels and their equilibrium swelling shape are illustrated in Scheme 1.

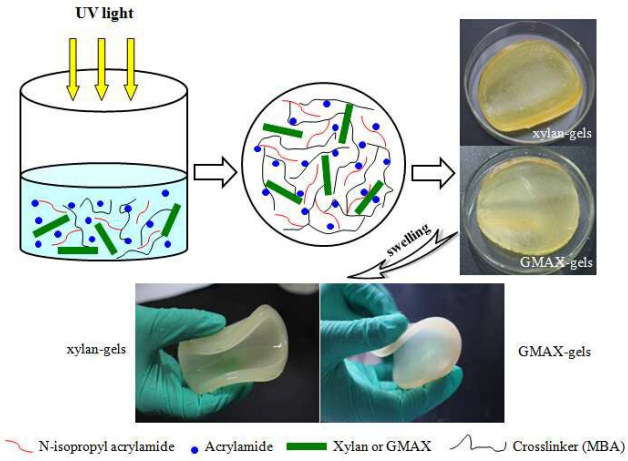

Scheme 1 The preparation scheme of xylan-gels and GMAX-gels and their equilibrium swelling shape.

The swelling behavior of hydrogels

The equilibrium swelling experiments were performed by the gravimetric method

under the conditions of buffer solution with desired pH at different temperatures. Hydrogels were swelling in the buffer solution in the temperature range from 25 ^{o}C to 37 ^{o}C. All samples were dried in vacuum oven at 50 ^{o}C to a constant weight. The dried hydrogels were submerged in the buffer solution to reach the equilibrium swelling state. The swollen samples were weighted after the surface moisture was removed by filter paper. The ionic strength of the solution was kept constant at 0.5 M using NaCl to adjust. The tests of all samples were conducted in triplicate. The swelling ratio (SR) and the equilibrium swelling ratio (S_{eq}) were calculated as follows:

$$SR = \frac{W_t - W_d}{W_d} \quad (2)$$

$$S_{eq} = \frac{W_{eq} - W_d}{W_d} \quad (3)$$

where W_t is the weight of swelling hydrogels, W_d is the initial weight of dried hydrogels and W_{eq} is the equilibrium weight during the swelling process.

Morphology of hydrogels

Scanning electron microscopy (SEM, Hitachi S3700, Japan) was used to observe the morphology of hydrogels at an acceleration voltage of 10 kV. The samples with a uniform thickness were fixed on a metal stub using carbon tape and coated with thin layer gold using an Agar HR sputter coater prior to testing.

Compressive stress measurement

Compressive stress measurement was conducted using an electromechanical material testing machine (Instron Universal Testing Machine, model 5565, USA) fitted with a 200 N load cell and a cross head speed of 2 mm/min. To reduce the influence of surface evenness, the cylindrical hyrogels with 4 cm diameter and 4 cm height were

preloaded with 1 N load. The hydrogel samples were in the hydrated state at 37 ^{o}C prior to measurement. The testing was performed at room temperature (25 ^{o}C and 50% humidity).

FTIR analysis

FTIR spectra were measured on a Fourier transform spectrophotometer (Nicolet 750, Florida, USA). The absorbance spectrum (4000–400 cm^{-1}) was acquired at 4 cm^{-1} resolution and recorded for a total of 32 scans. Hydrogels were dried to constant weight in a vacuum oven at 50 ^{o}C, and then the 1% finely ground hydrogel samples were mixed with KBr to be pressed into a plate for measurement.

Thermogravimetric analysis (TGA)

The thermodynamic properties of these hydrogels were monitored using thermogravimetric analysis on a simultaneous thermal analyzer (TGA Q500, TA Instruments, New Castle, DE, USA). Hydrogel samples of approximately 9~11 mg were cut into pieces and heated from room temperature to 700 ^{o}C at a 10 ^{o}C/min heating rate under a nitrogen flow of 20 mL/min.

X-ray diffraction (XRD) measurement

X-ray patterns of xylan, GMAX, xylan-based hydrogels were analyzed using an X-ray diffractometer (Bruker, model D8 advance, Germany) with Cu Kα radiation at a voltage of 40 kV and 40 mA. The measurements were made with scattering angles of 5–60° and a scanning speed of 2°/min.

Differential scanning calorimetry (DSC) measurement

The lower critical solution temperature (LCST) of hydrogels was determined by differential scanning calorimetry (DSC Q200, USA) analysis. The thermal analyses were performed from 10 ^{o}C to 55 ^{o}C on the swollen hydrogel samples under a dry nitrogen atmosphere with a flow rate of 25.0 mL/min and heating rate of 5 ^{o}C/min and then were cooled down to room temperature.

Preparation of hydrogels loaded by acetylsalicylic acid

Dried hydrogels were placed in the 100% w/w ethanol solution containing 10% (w/v) acetylsalicylic acid, for 24-h loading in the darkness. Ethanol in hydrogels was evaporated in a vacuum oven. Hydrogels loaded with acetylsalicylic acid turned white after the removal of ethanol and then weighed the drug-loaded hydrogels. The dried drug-loaded hydrogels were stored in a desiccator. The acetylsalicylic acid loading amount and the encapsulation efficient were determined by following equation:

$$\text{Drug loading (\%)} = \frac{W_d}{W_h} \times 100 \quad (4)$$

$$\text{Encapsulation efficiency (\%)} = \frac{W_a}{W_m} \times 100 \quad (5)$$

where W_d is the total weight of drug in hydrogels and W_h is the total weight of dried hydrogels. W_a refers to the actual drug loading weight and W_m is the theoretical maximum drug loading weight.

***In vitro* drug release**

Drug release experiments were performed in a horizontal oscillator at a shaking speed of 50 rpm at 37 ^{o}C. The drug-loaded hydrogels were placed in a buffer solution. Five milliliters of each solution was collected at 1 h intervals for the determination of drug content using a UV/Vis spectrophotometer (SHIMADZU UV1800, Japan) at 296 nm,

and an equal volume of the same solution medium was added back to maintain a constant volume. All samples were conducted in triplicate in vitro release tests. The concentration of the drug in the different buffer solutions was calculated by the following calibrated standard curves:

pH 1.2: y = 0.0032x + 0.0045 (r = 0.999),

pH 7.4: y = 0.00245x + 0.0356 (r = 0.999).

The percentage of drug released from hydrogels was calculated by the following formula:

$$\text{Cumulative release}\,(\%) = \frac{W_{dt}}{W_{\infty}} \times 100 \qquad (6)$$

where W_{dt} is the weight of released drug at time t and W_{∞} is the total weight of loaded drug in hydrogels.

Cell viability assay

The cell viability assay was performed by MTT method using NIH3T3 cells. Hydrogels were tailored to a disk with the diameter of 15 mm and sterilized by γ-ray before cells were cultured. NIH3T3 cells (5×10^3 cells per well) were seeded on the surface of hydrogels with 10% FBS and incubated at 37 ºC in a 5% CO_2 humidified atmosphere for 24 h and 72 h (The culture medium was replaced every day). Then the medium was removed. Fresh medium (1 mL) and MTT (100 μL, 5 mg·mL^{-1}) were added to each well, followed by 4 h of incubation at 37 ºC. Subsequently, the supernatant was carefully removed, and 1 ml of DMSO was added to each well to dissolve the formazan precipitate. The absorbance of the solution was measured with micro-plate reader (Bio-Rad 550, USA) at 492 nm to determine the Optical Density (OD) value. The well without hydrogel samples was used as a control group. Each group was tested three times. The cell viability was evaluated by the MTT assay and

calculated as follows:

$$\text{Cell viability} = \frac{OD_{gel}}{OD_{ctrl}} \times 100\% \quad (7)$$

where OD_{gel} is the optical density of cells cultured on hydrogels, OD_{ctrl} is the optical density of the blank control group.

Results and Discussion

Swelling behavior analysis of xylan-gels and GMAX-gels

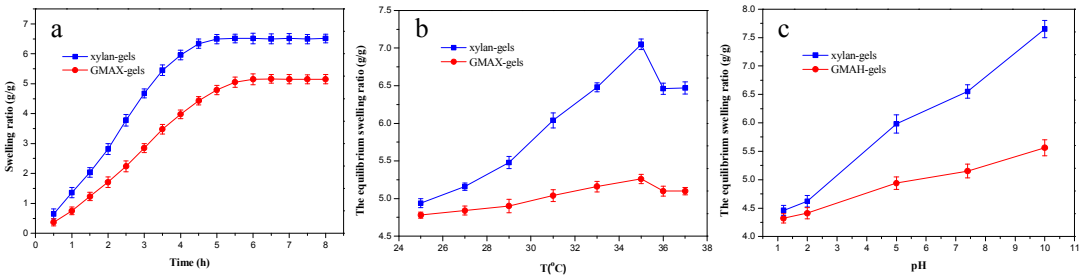

Fig. 1 (a) The swelling ratio of xylan-gels and GMAX-gels as a function of time, (b) The S_{eq} of xylan-gels and GMAX-gels as a function of temperature in neutral pH and (c) The S_{eq} of xylan-gels and GMAX-gels as a function of pH (pH 1.2, 2.0, 5.0, 7.4, 10.0) at 37 °C.

The swelling ratio is a crucial parameter to evaluate the swelling capacity of hydrogels. Fig. 1 (a) shows the swelling ratio (SR) of xylan-gels and GMAX-gels as a function of time in the neutral solution. For xylan-gels, the SR increased quickly during the first 3 h and then gradually got into slow trend. The equilibrium swelling of xylan-gels was obtained after 5 h. In comparison, the SR of GMAX-gels slowly increased, and it took 6 h to reach the equilibrium swelling. The equilibrium swelling ratios (S_{eq}) of xylan-gels and GMAX-gels were 6.51 and 5.15, respectively.

The S_{eq} of xylan-gels and GMAX-gels at different temperatures are illustrated in

Fig. 1 (b). Both S_{eq} of xylan-gels and GMAX-gels had the same trend of first increase then decrease and the maximum values occurred at 35 ^{o}C. This indicated the LCST of these hydrogels existed in the vicinity of 35 ^{o}C and hydrogels shrinked sharply after 35 ^{o}C which led to the lower equilibrium swelling ratio. For xylan-gels, the S_{eq} increased steadily from 4.94 to 7.05 before 35 ^{o}C and reduced sharply to 6.46 at 36 ^{o}C. With a further increment of temperature to 37 ^{o}C (approximately the temperature of the human body), the S_{eq} had a slight increase. While the S_{eq} of GMAX-gels increased slowly before 29 ^{o}C and then swelled up nearly in the proportion to the increment of temperature from 29 ^{o}C to 35 ^{o}C. There was no obvious change between 36 ^{o}C and 37 ^{o}C. In addition, the maximum of the S_{eq} for GMAX-gels was 5.26, which was lower than that of xylan-gels. It was explained that GMAX-gels had more compact network structure than xylan-gels due to the high reactivity between GMAX and monomers after introducing methacryloyl groups onto the native xylan backbone. In most cases, hydrogels with higher cross-linking density caused an appreciable decrease in swelling capacity.[8,46] GMAX was highly more reactive than xylan because of alkenyl-functional groups onto xylan. Therefore, to improve the reactivity of hemicelluloses, some researchers had attempted to introduce alkenyl groups onto the backbone of hemicelluloses.[26,47,48]

Fig. 1 (c) shows the S_{eq} of xylan-gels and GMAX-gels as a function of pH at 37 ^{o}C. Obviously, the S_{eq} of the two kinds of hydrogels increased along with the increase of pH from 1.2 to 10 due to the changes of intermolecular forces and the swelling osmotic pressure. The maximum S_{eq} of xylan-gels and GMAX-gels were 7.65 and 5.56, respectively. Moreover, in the simulated gastric environment (pH 1.2), the S_{eq} of xylan-gels and GMAX-gels were 4.46 and 4.32, respectively, which were much lower than those in the simulated intestinal fluids (6.55 and 5.15 at pH 7.4 for xylan-gels

and GMAX-gels). When the pH value reached to alkaline condition, the swelling ratios for xylan-gels and GMAX-gels rapidly increased which could be interpreted that ionization of –OH groups on xylan with the increased pH values enlarged the space in the networks due to the electrostatic repulsions in alkaline condition. While in acidic environment, the formation of hydrogen bonds in the hydrogels matrix and solution system restrained the swelling behaviors of hydrogels.[39] Xylan-gels had higher S_{eq} than GMAX-gels due to the difference of the crosslinking density between hydrogel networks.

The morphologic structure and compressive properties

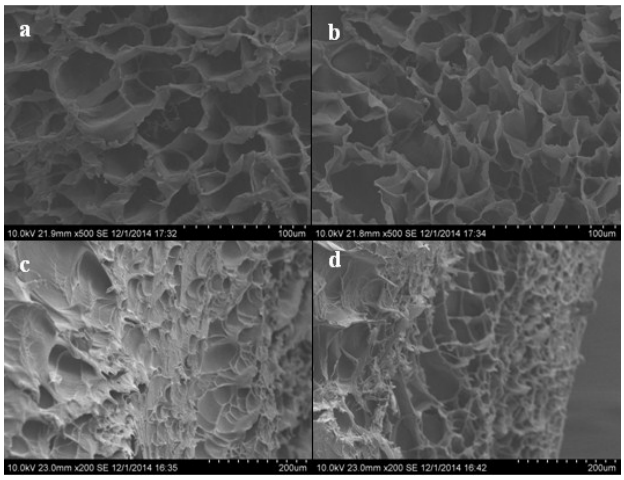

Fig. 2 SEM surface (a and b) and cross section (c and d) images of freeze-dried xylan-gels (left) and GMAX-gels (right), the hydrogel samples were conditioned at 37 ^{o}C before freeze-drying.

SEM micrographs of the surface and cross sections of xylan-gels and GMAX-gels are illustrated in Fig. 2. Obviously, it was observed that both xylan-gels and GMAX-gels displayed porous structures like honeycomb. However, GMAX-gels exhibited more

homogeneous and denser porous architecture while xylan-gels showed the relatively macroporous structure and uneven mass distribution, indicating GMAX-gels had higher crosslinking density. This conclusion was in accordance with the equilibrium swelling ratios of xylan-gels and GMAX-gels. The cross section micrographs could reflect the degree of crosslinking interactions and polymerization of the internal structure, from which more holes were observed in the structure of GMAX-gels. While xylan-gels had more irregular dents and partial collapse in the structure of the cross section, which might result from the differences in the stress tolerance of the networks between xylan-gels and GMAX-gels after slicing and freeze-drying samples. This was also indicative of the instability and brittleness of xylan-gels relatively, which would be further proved by the following compressive tests.

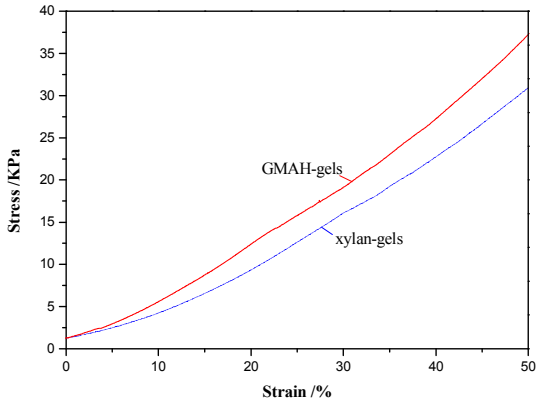

Fig. 3 Compressive stress-strain curves of xylan-gels and GMAX-gels.

Compression stress test was measured to evaluate the density of hydrogels networks.[49] The stress-strain curves of hydrogels in Fig. 3 almost had a linear type of growth curve. The compressive moduli of xylan-gels and GMAX-gels were 105.17 kPa and 156.78 kPa, respectively, as showed in Table 1. In Fig. 3, the compressive properties of GMAX-gels had an apparent advantage especially when the strain

increased. When the strain reached to 50%, the stress of GMAX-gels reached to 37.03 kPa, while the stress of xylan-gels was 30.99 kPa. This was indicative of stronger intermolecular forces and higher crosslinking density in the GMAX-gels structure than xylan-gels, which was consistent with the results of SEM and swelling properties. The xylan-based hydrogels possessing notable compressive properties have the promising application as drug loaded carriers. Stachowiak *et al.* prepared the porous polyethylene glycol gels by templating on a colloidal crystal.[50] The maximum of compressive modulus of gels was 22.6 kPa. Although the strength values were not reported, the gels were described as ‘‘robust’’ and the porous structure might certainly be expected to withstand significant amounts of stress.

FTIR analysis of xylan, GMAX and prepared hydrogels

Fig. 4 (a) exhibits the FTIR spectra of xylan, GMAX and prepared hydrogels. The broad band at 3431 cm^{-1} originates from the stretching of –OH groups on xylan. Meanwhile, the intensity of GMAX-gels, xylan-gels and GMAX at 3431 cm^{-1} became lower remarkably which indicated that the chemical reaction of hydroxyl groups on xylan occurred. The absorption bands at 3431, 2923, 1624, 1400, 1254, 1162, 1112, 1081, 1045, 985, and 893 cm^{-1} are associated with xylan.[33,51] The prominent band at 1045 cm^{-1} originates from the C–O–C stretching of pyranoid-ring xylans.[17] A sharp band at 893 cm^{-1} is assigned to β-glucosidic linkages between the xylose units. The band at 2923 cm^{-1} is assigned to the C−H stretching vibration of alkane in xylan molecular structure. The bands at 1721 cm^{-1} and 1635 cm^{-1} in the spectrum of GMAX are attributed to stretching vibrations of C=O (in ester group) and C=C originated from GMA.[26] Furthermore, a small band at 3223 cm^{-1} is present, which is most likely from =C–H groups originated from GMA. Compared to the spectrum of xylan, a new

sharp unsaturated C–H (=C–H) bending vibration appears at 807 cm^{-1} in the spectrum of GMAX. This indicated that methacryloyl groups were introduced to xylan chains successfully.[38] In the spectra of xylan-gels and GMAX-gels, no peaks is present at 807 cm^{-1} which confirmed that the monomers (AM and NIPAm) and corsslinker (MBA) had reacted completely. The strong characteristic absorption bands at 3187 cm^{-1} and 1640 cm^{-1} are assigned to N–H asymmetric stretching vibration peak (from PNIPAm) and amide carbonyl groups in PNIPAm and PAM,[48,52] respectively (N-H stretch from PAM, overlap). The new band at 1122 cm^{-1} originates from C–N stretching vibrations of aliphatic amide. These results indicated that GMA, NIPAm and other monomers were actually grafted onto the backbone of xylan, which supported the formation of copolymers.

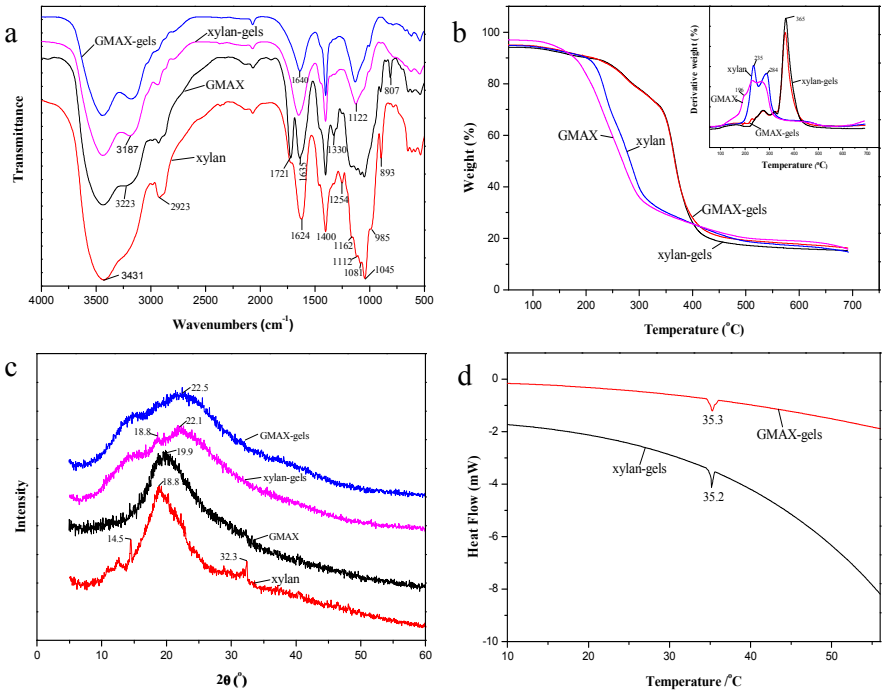

Fig. 4 (a) FTIR spectra of the GMAX-gels, xylan-gels, GMAX and xylan; (b) TGA and DTGA curves of xylan, GMAX, xylan-gels and GMAX-gels; (c) X-ray diffractions of GMAX-gels, xylan-gels, GMAX and xylan; (d) DSC curves of GMAX-gels and xylan-gels.

Thermogravimetric analysis

Thermogravimetric analysis is a standard parameter to determine the thermal stability of materials. Fig. 4 (b) shows the TGA and DTGA curves of xylan, xylan-gels and GMAX-gels. For xylan and GMAX, the weight loss below 200 ^{o}C was attributed to the degradation of water. And then the degradation rate of GMAX was faster than that of xylan owing to the attached methacryloyl groups and the change of the molecular weight after the modification of xylan. However, xylan had greater weight loss than GMAX after 400 ^{o}C. This indicated GMAX had stronger intermolecular forces than xylan. In the DTGA curves, the typical degradation peaks of xylan were observed at 235 ^{o}C and 284 ^{o}C, while the degradation peak of GMAX weakened greatly and shifted at 231 ^{o}C and 262 ^{o}C due to structural changes. A new small degradation peak occurring at 196 ^{o}C was attributed to the destruction of hydrogen bond with evaporation of water. The weight losses of xylan-gels and GMAX-gels were divided into the following four stages: below 220 ^{o}C, 220-340 ^{o}C, 340-400 ^{o}C and 400-700 ^{o}C. There was no difference between the two kinds of hydrogels before 400 ^{o}C. The weight loss of hydrogels resulting from the water evaporation and small molecules degradation occurred below 220 ^{o}C. The weight loss between 220 ^{o}C and 400 ^{o}C was owing to the degradation of xylan chains. The carbonation of the copolymer matrix occurred after 400 ^{o}C. Xylan-gels had lower thermal stability than GMAX-gels in the later period, which was in accordance with the thermogravimetric results of xylan and GMAX. In addition, it was observed that the degradation peak of xylan-gels was stronger at 365 ^{o}C which was indicative of the existence of denser and solider network structure in GMAX-gels.

X-ray diffraction (XRD) analysis

The X-ray diffractions of xylan, GMAX, xylan-gels and GMAX-gels are shown in Fig. 4 (c). As observed, a broad diffraction peak at $2\theta=18.8^{o}$ is typically attributed to xylan, and small sharp diffraction peaks at $2\theta=14.5^{o}$ and 32.3^{o} indicated xylan had better crystalline structure than the amorphous xylan-type hemicelluloses studied by Peng *et al.* and Chen *et al.*[53,54] The peaks at 14.5^{o} and 32.3^{o} disappeared in the diffraction pattern of GMAX and the reflection at 18.8^{o} shifted to 19.9^{o} which implied the transesterification reaction of xylan in the DMSO system had a significant impact on the crystalline structural changes of xylan. In the intensity patterns of hydrogels, the peak at $2\theta=18.8^{o}$ for GMAX-gels disappeared and also significantly decreased in the pattern of xylan-gels. Simultaneously, a new peak emerged at around $2\theta=22^{o}$, which was due to the destruction of intermolecular hydrogen bonds after the crosslinking and copolymerization of the monomers (NIPAm, AM and MBA) with xylan and GMAX. The results indicated that the grafting copolymerization led to the destruction of the crystalline structure of the native xylan.

Differential scanning calorimetry measurement

The LCST of temperature sensitive hydrogels is determined by DSC in Fig. 4 (d). The peak of GMAX-gels was broader than that of xylan-gels which suggested the stronger networks decelerated the volume phase transition. The LCST emerged at a little higher than 35 ^{o}C for GMAX-gels and xylan-gels. Therefore, these xylan-based hydrogels showed higher LCST than pure PNIPAm hydrogels at around 33 ^{o}C. This could be explained that addition of biopolymers increased the hydrophilicity of the whole hydrogels networks owing to a large quantity of hydrophilic hydroxyl groups

of xylan which increased the combination of intermolecular forces especially the hydrogen bonds between the hydrogels matrix and water molecules.[23] PAM also increased interactions of hydrogen bonds due to the amide groups. Additionally, hydrogen bonds breaking requires more energy which would greatly enhanced the transition temperature of LCST.[55] Zhang *et al.* obtained the same conclusion that the LCST increased with the increasing biopolymer contents for modified dextran/PNIPAm hydrogels.[23] The balance of hydrophilicity/hydrophobicity in the PNIPAm hydrogels induced temperature sensitive properties.[56] The incorporation of xylan, GMAX and PAM had a significant impact on the phase transition. Absorbed water in the network of hygrogels could exist in three states: bound water, half-bond water, and free water. Free water was easier to remove compared with bound and half-bond water.[57] The volume of hydrogels would shrink sharply as the free water was dislodged owing to the decrease of intermolecular forces when the temperature exceeded LCST, which was consistent to the results of the swelling behavior in Fig. 1 (a). Hydrogels with LCST close to the body temperature have the potential application as the carrier for drug controlled release in biomedical field.

***In vitro* drug release of xylan-gels and GMAX-gels**

The cumulative drug release behaviors from the drug-loaded hydrogels in simulated gastric (pH 1.2) and intestinal (pH 7.4) fluids at 37 ^{o}C are shown in Fig. 5. Acetylsalicylic acid has been extensively used as anti-platelet drug for the prevention of cardiovascular events.[40,41] In our study, it was used as the model drug to determine the drug controlled release of xylan-gels and GMAX-gels. The drug loading of xylan-gels and GMAX-gels showed in Table 1 were 28.65% and 35.56%, respectively. The drug encapsulation efficiency of xylan-gels and GMAX-gels were 64.46% and

95.21%. This indicated that GMAX-gels had stronger drug encapsulation properties than xylan-gels. This could be interpreted that GMAX-gels which had low pore diameter and well-ordered networks provided more electrostatic interaction for acetylsalicylic acid. While irregular internal structure of xylan-gels had lower affinity and electrostatic interaction.[58]

In the Fig. 5 (a), the cumulative drug release rate of xylan-gels in the simulated intestinal fluids (pH 7.4) was increased fast at the initial 4 hours and then increased slowly. The drug release percentage was achieved to the maximum 77.5% when the release time was 6 h. While in the simulated gastric fluids (pH 1.2), the drug release percentage was restrained and the drug release took 6 h to reach equilibrium (45.6%). The formation of hydrogen bonds complex in an acid medium was responsible for restricting the mobility of network of hydrogels.[23] In the same way, a lower S_{eq} of hydrogels was found under the acidic condition in Fig. 1 (c). In the intestinal fluids, the ionization of –OH groups on xylan enlarged the space in the hydrogels networks and increased the drug release of hydrogels due to the electrostatic repulsions and changed the swelling osmotic pressure between the hydrogel phase and the external solution.[59] The interactions between functional groups of polymers and drugs, such as electrostatic interactions and hydrogen bonds had a significant effect on drug delivery in different environment. Li *et al.* and Tian *et al.* got the same conclusions.[60,61] In comparison, the drug release percentage of GMAX-gels had a well-ordered increase and the drug could release continuously up to 8 h in Fig. 5 (b). The appropriate sustained-release time of drugs was of great significance which would improve the curative effect and relieve the side effect of high dose drugs. The maximum drug release percentage of GMAX-gels was 84.2% at pH 7.4, superior to the release percentage of xylan-gels. In the gastric fluids, drug release percentage of GMAX-gels

was 34.6%. Moreover, low gastric drug release could reduce the adverse effects of acetylsalicylic acid. To verify whether acetylsalicylic acids were hydrolyzed or not, chromogenic reaction was conducted. Salicylic acid and acetic acid were hydrolyzates of acetylsalicylic acids. The former could be identified by the chromogenic reaction using ferric chloride ($FeCl_3$). The results showed that no chromogenic reaction happened in the solution after the drug release, which indicated acetylsalicylic acids were not hydrolyzed in xylan-gels and GMAX-gels. The xylan-based hydrogels containing the remained acetylsalicylic acids could be removed from the patient body along with the excreta. Overall, both xylan-gels and GMAX-gels had desired drug release rates in the simulated intestinal fluids. GMAX-gels had higher encapsulation efficiency and lower gastric drug release and showed promising application as acetylsalicylic acid carriers in the intestinal targeted drug delivery.

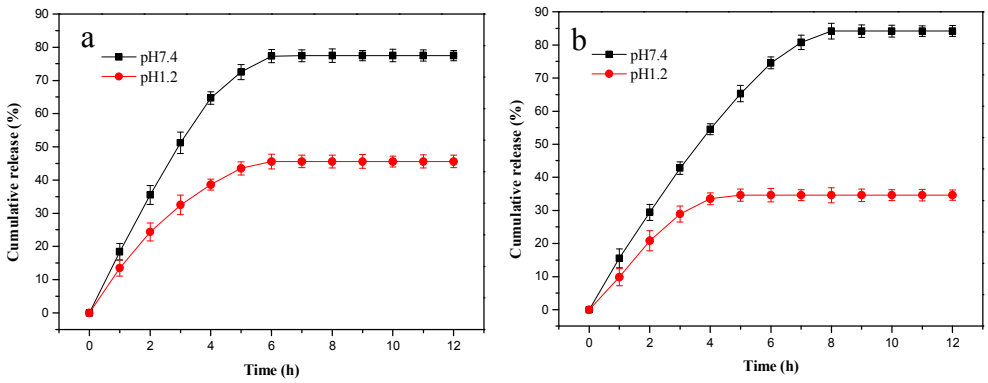

Fig. 5 In vitro cumulative drug release from the drug-loaded xylan-gels (a) and GMAX-gels (b) in simulated gastric (pH 1.2) and intestinal (pH 7.4) fluids at 37 °C.

Cytocompatibility studies of xylan-gels and GMAX-gels

NIH3T3 cells were employed as model cells for evaluating the cytocompatibility of xylan-gels and GMAX-gels by MTT method.[21,62] As shown in Fig. 6, after incubation

in culture medium for 24 h, the cell viability of NIH3T3 cells was 105% and 106% for xylan-gels and GMAX-gels, respectively. Moreover, the cell viability was further increased to 115% and 121% after 72 h. In comparison, the cell viability of the GMAX-gels and xylan-gels was similar after 24 h incubation. GMAX-gels had higher cell viability than xylan-gels with prolonging incubation time. This could be attributed to more stable network structure of GMAX-gels. All cellular viability values of hydrogels were higher than 100%, indicating that xylan-based hydrogels had non-cytotoxicity against NIH3T3 cells. This result confirmed the great proliferative potential of NIH3T3 cells on xylan-based hydrogels, implying that these hydorgles would have the promising application as oral drug delivery carriers.

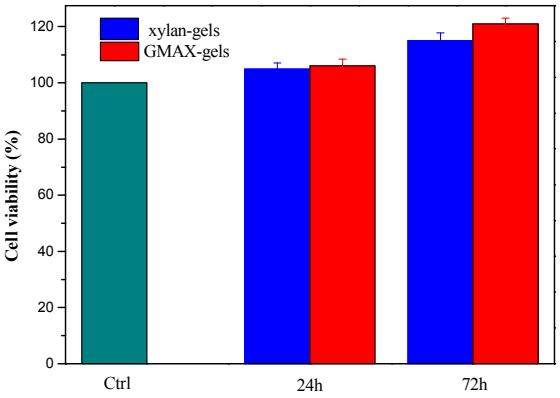

Fig. 6 NIH3T3 cell viability of xylan-gels and GMAX-gels by MTT assay at 37 ^{o}C after incubation for 24 h and 72 h.

Conclusions

In summary, temperature/pH dual-response xylan-based P(AM-co-NIPAm) hydrogels were prepared successfully by the grafting copolymerization under ultraviolet irradiation. Results indicated that introducing functional groups on xylan had the great impact on the properties of xylan-based hydrogels. The cumulative drug release

percentages of xylan-gels and GMAX-gels for acetylsalicylic acid as the potential anti-platelet drug were achieved to 77.5% and 84.2% in the intestinal fluids and their sustained release time in the pH 7.4 buffer solutions was maintained for 6 h and 8 h, respectively. GMAX-gels had higher drug cumulative release and longer release time in the intestinal fluids. Moreover, GMAX-gels showed strong the greater compressive property, the higher encapsulation efficiency (about 95.21%) and the lower drug release in gastric fluid, which could relieve side-effects for patients with long-term acetylsalicylic acid use. More importantly, it was demonstrated that both xylan-based hydrogels had the excellent cytocompatibility by cell viability assay and NIH3T3 cells in GMAX-gels had higher cell viability. Therefore, GMAX-gels with high sensitivity to temperature/pH and great drug release behaviors had a promising application as acetylsalicylic acid carriers in drug controlled release, especially in the intestinal targeted delivery.

Acknowledgments

This work was supported by grants from National Natural Science Foundation of China (No. 21406080), the Author of National Excellent Doctoral Dissertations of China (201169) and Science and Technology Planning Project of Guangdong Province (2013B010404004) and the Fundamental Research Funds for the Central Universities of SCUT (D2154620, 2014ZG0003).

References

1 W. E. Hennink and C. F. van Nostrum, *Adv. Drug Deliver Rev.*, 2002, **54**, 13–36.

2 T. Miyata, T. Uragami and K. Nakamae, *Adv. Drug Deliver Rev.*, 2002, **54**, 79–98.

3 N. A. Peppas and J. J. Sahlin, *Biomaterials*, 1996, **17**, 1553–1561.

4 A. S. Hoffman, *Adv. Drug Deliver Rev.*, 2002, **54**, 3–12.

5 K. Y. Lee and D. J. Mooney, *Chem. Rev.*, 2001, **101**, 1869–1880.

6 M. V. Sefton, M. H. May, S. Lahooti and J. E. Babensee, *J. Controlled Release*, 2000, **65**, 173–186.

7 Y. Qiu and K. Park, *Adv. Drug Deliver Rev.*, 2012, **64**, 49−60.

8 X. Z. Zhang, D. Q. Wu and C. C. Chu, *Biomaterials*, 2004, **5**, 3793–3805.

9 G. Fundueanu, M. Constantin and P. Ascenzi, *Biomaterials*, 2008, **29**, 2767–2775.

10 H. Ichikawa and Y. Fukumori, *J. Controlled Release*, 2000, **63**, 107–119.

11 X. Z. Zhang and C. C. Chu, *Polymer*, 2005, **46**, 9664–9673.

12 J. H. Kim, S. B. Lee, S. J. Kim and Y. M. Lee, *Polymer*, 2002, **43**, 7549–7558.

13 J. S. Park, H. N. Yang, D. G. Woo, S. Y. Jeon and K. H. Park, *Biomaterials*, 2013, **34**, 8819–8834.

14 T. Tanaka, D. Fillmore, S. T. Sun, I. Nishio, G. Swislow and A. Shah, *Phys. Rev. Lett.*, 1980, **45**, 1636–1639.

15 B. Kim and N. A. Peppas, *Macromolecules*, 2002, **35**, 9545–9550.

16 M. D. Kurkuri and T. M. Aminabhavi, *J. controlled release*, 2004, **96**, 9–20.

17 X. F. Sun, H. L. Wang, Z. X. Jing and R. Mohanathas, *Carbohydr. Polym.*, 2013, **92**, 1357–1366.

18 M. S. Bostan, M. Senol, T. Cig, I. Peker, A. C. Goren, T. Ozturk and M. S. Eroglu, *Int. J. Biol. Macromol.*, 2013, **52**, 177–183.

19 G. Y. Li, L. Guo, X. J. Chang and M. Y. Yang, *Int. J. Biol. Macromol.*, 2012, **50**, 899–904.

20 A. Hebeish, S. Farag, S. Sharaf and T. I. Shaheen, *Carbohydr. Polym.*, 2014, **102**, 159–166.

21 C. Cheng, D. D. Xia, X. L. Zhang, L. Chen and Q. Q. Zhang, *J. Mater. Sci.*, 2015, **50**, 4914–4925.

22 S. Bettini, V. Bonfrate, Z. Syrgiannis, A. Sannino, L. Salvatore, M. Madaghiele, L. Valli and G. Giancane, *Biomacromolecules*, 2015, **16**, 2599−2608.

23 X. Z. Zhang, D. Q. Wu and C. C. Chu, *Biomaterials*, 2004, **25**, 4719–4730.

24 A., Ebringerova and T. Heinze, *Macromol. Rapid Comm.*, 2000, **21**, 542–556.

25 E. Noaman, N. K. B. El-Din, M. A. Bibars, A. A. Abou Mossallam and M. Ghoneum, *Cancer Lett.*, 2008, **268**, 348–359.

26 X. F. Cao, X.W. Peng, L. X. Zhong and R. C. Sun, *J. Agric. Food Chem.*, 2014, **62**, 10000−10007.

27 A. Ebringerova, Z. Hromadkova and T. Heinze, *Adv. Polym. Sci.*, 2005, **186**, 1–67.

28 A. Barbat, V. Gloaguen, C. Moine, O. Sainte-Catherine, M. Kraemer, H. Rogniaux, D. Ropartz and P. Krausz, *J. Nat. Prod.*, 2008, **71**, 1404–1409.

29 E. E. Oliveira, A. E. Silva, T. N. Junior, M. C. S. Gomes, L. M. Aguiar, H. R. Marcelino, I. B. Araujo, M. P. Bayer, N. M. P. S. Ricardo, A. G. Oliveira and E. S. T. Egito, *Bioresour. Technol.*, 2010, **101**, 5402–5406.

30 Z. Hromadkova, J. Kovacikova and A. Ebringerova, *Ind. Crops Prod.*, 1999, **9**, 101–109.

31 A. Ebringerova, A. Kardosova, Z. Hromadkova, A. Malovikova and V. Hribalova, *Int. J. Biol. Macromol.*, 2002, **30**, 1–6.

32 V. Kuzmenko, D. Hagg, G. Toriz and P. Gatenholm, *Carbohydr. Polym.*, 2014, **102**, 862–868.

33 X. W. Peng, J. L. Ren, L. X. Zhong, F. Peng and R. C. Sun, *J. Agric. Food Chem.*, 2011, **59**, 8208–8215.

34 M. S. Lindblad, E. Ranucci and A. C. Albertsson, *Macromol. Rapid Comm.*, 2001, **22**, 962–967.

35 J. Voepel, U. Edlund and A. C. Albertsson, *J. Polym. Sci., Part A: Polym.Chem.*, 2009, **7**, 3595–3606.

36 L. Jennie Baier, K. A. Bivens, C. W. Patrick and C. E. Schmidt, *Biotechnol. Bioeng.*, 2003, **82**, 578–89.

37 J. Trudel and S. P. Massia, *Biomaterials*, 2002, **23**, 3299–3307.

38 X. W. Peng, J. L. Ren, L. X. Zhong, R. C. Sun, W. B. Shi and B. J. Hu, *Cellulose*, 2012, **19**, 1361–1372.

39 L. Chen, J. Dong, Y. M. Ding and W. J. Han, *J. Appl. Polym. Sci.*, 2005, **96**, 2435–2439.

40 J. H. Han, J. M. Krochta, M. J. Kurth and Y. L. Hsieh, *J. Agric. Food Chem.*, 2000, **48**, 5278–5282.

41 M. Otsuka, Y. Matsuda, Y. Suwa, J. L. Fox and W. I. Higuchi, *Am. J. Pharmacol. Sci.*, 1994, **83**, 259–263.

42 K. Kent, M. Ganetsky, J. Cohen and S. Bird, *Clin. Toxicol.*, 2009, **46**, 297–299.

43 M. S. Khalil, *Histol. Histopathol.*, 2015, **30**, 855–864.

44 K. Schwikal, T. Heinze, A. Ebringerova and K. Petzold, *Macromol. Symp.*, 2006, **232**, 49–56.

45 C. Vaca-Garcia, M. E. Borredon and A. Gaseta, *Cellulose*, 2001, **8**, 225–231.

46 K. Kabiri, H. Omidian, S. A. Hashemi and M. J. Zouhuriaan-Mehr, *Eur. Polym. J.*, 2003, **39**, 1341–1348.

47 M. S. Lindblad, A. Albertsson, E. Ranucci, M. Laus and E. Giani, *Biomacromolecules*, 2005, **6**, 684–690.

48 J. Y. Yang, X. S. Zhou and J. Fang, *Carbohydr. Polym.*, 2011, **86**, 1113–1117.

49 J. A. Stammen, S. Williams, D. N. Ku and R. E. Guldberg, *Biomaterials*, 2001, **22**, 799–806.

50 A. N. Stachowiak, A. Bershteyn, E. Tzatzalos and D. J. Irvine, *Adv. Mater.*, 2005, **17**, 399.

51 J. M. Fang, R. C. Sun, J. Tomkinson and P. Fowler, *Carbohydr. Polym.*, 2000, **41**, 379–387.

52 H. Wei, X. Z. Zhang, C. Cheng, S. X. Cheng and E. X. Zhuo, *Biomaterials*, 2007, **28**, 99–107.

53 X. W. Peng, J. L. Ren, L. X. Zhong and R. C. Sun, *Biomacromolecules*, 2011, **12**, 3321–3329.

54 W. Chen, L. X. Zhong, X. W. Peng, K. Wang, Z. F. Chen and R. C. Sun, *Catal. Sci. Technol.*, 2014, **4**, 1426–1435.

55 L. X. Zhong, X. W. Peng, D. Yang, X. F. Cao and R. C. Sun, *J. Agric. Food Chem.*, 2013, **61**, 655–661.

56 X. J. Pan and Y. Sano, *Bioresour. Technol.*, 2005, **96**, 1256–1263.

57 S. Zhang, Y. Guan, G. Q. Fu, B. Y. Chen, F. Peng, C. L. Yao and R. C. Sun, *J. Nanomater.*, 2014, http://dx.doi.org/10.1155/2014/675035.

58 P. Mukhopadhyay, K. Sarkar, S. Bhattacharya, A. Bhattacharyya, R. Mishra and P. P. Kundu, *Carbohydr. Polym.*, 2014, **112**, 627–637.

59 H. Mittal, R. Jindal, B. S. Kaith, A. Maity and S. S. Ray, *Carbohydr. Polym.*, 2015, **115**, 617–628.

60 G. Li, S. Song, L. Guo and S. Ma, *J. Polym. Sci. A: Polym. Chem.*, 2008, **46**, 5028–5035.

61 Y. Tian, L. Bromberg, S. N. Lin, T. A. Hatton and K. C. Tam, *J. Control. Release*, 1 2007, **121**, 137–145.

62 Y. H. Lien, T. M. Wu, J. H. Wu and J. W. Liao, *J. Nanopart. Res.*, 2011, **13,**

5065–5075.